LETTERS

Reduced mixing generates oscillations and chaos in the oceanic deep chlorophyll maximum

Jef Huisman[1]*, Nga N. Pham Thi[2]*, David M. Karl[3] & Ben Sommeijer[2]

Deep chlorophyll maxima (DCMs) are widespread in large parts of the world's oceans[1–7]. These deep layers of high chlorophyll concentration reflect a compromise of phytoplankton growth exposed to two opposing resource gradients: light supplied from above and nutrients supplied from below. It is often argued that DCMs are stable features. Here we show, however, that reduced vertical mixing can generate oscillations and chaos in phytoplankton biomass and species composition of DCMs. These fluctuations are caused by a difference in the timescales of two processes: (1) rapid export of sinking plankton, withdrawing nutrients from the euphotic zone and (2) a slow upward flux of nutrients fuelling new phytoplankton production. Climate models predict that global warming will reduce vertical mixing in the oceans[8–11]. Our model indicates that reduced mixing will generate more variability in DCMs, thereby enhancing variability in oceanic primary production and in carbon export into the ocean interior.

In oligotrophic waters, where the surface mixed layer is depleted of nutrients, subsurface maxima in chlorophyll concentration and phytoplankton biomass are often found (Fig. 1). Such deep chlorophyll maxima are permanent features in large parts of the tropical and subtropical oceans[1–5]. Furthermore, seasonal DCMs commonly develop in temperate regions[4,6] and even in the polar oceans[7] when nutrients are depleted in the surface layer with the onset of the summer season. It is generally believed that DCMs are stable features, tracking seasonal changes in light and nutrient conditions. However, here we extend recent phytoplankton models[12–16] to show that the phytoplankton populations of DCMs can show sustained fluctuations.

Consider a vertical water column. Let z indicate the depth in the water column. Let P denote the phytoplankton population density (number of cells per m^3). The population dynamics of the phytoplankton can be described by a reaction–advection–diffusion equation[12–17]:

$$\frac{\partial P}{\partial t} = \text{growth} - \text{loss} - \text{sinking} + \text{mixing}$$

$$= \mu(N,I)P - mP - v\frac{\partial P}{\partial z} + \kappa\frac{\partial^2 P}{\partial z^2} \qquad (1)$$

where $\mu(N,I)$ is the specific growth rate of the phytoplankton as an increasing saturating function of nutrient availability N and light intensity I, m is the specific loss rate of the phytoplankton, v is the phytoplankton sinking velocity, and κ is the vertical turbulent diffusivity. The nutrient dynamics in the water column can be described as[12–14]:

$$\frac{\partial N}{\partial t} = -\text{uptake} + \text{recycling} + \text{mixing}$$

$$= -\alpha\mu(N,I)P + \varepsilon\alpha mP + \kappa\frac{\partial^2 N}{\partial z^2} \qquad (2)$$

where α is the nutrient content of the phytoplankton, and ε is the proportion of nutrient in dead phytoplankton that is recycled. We

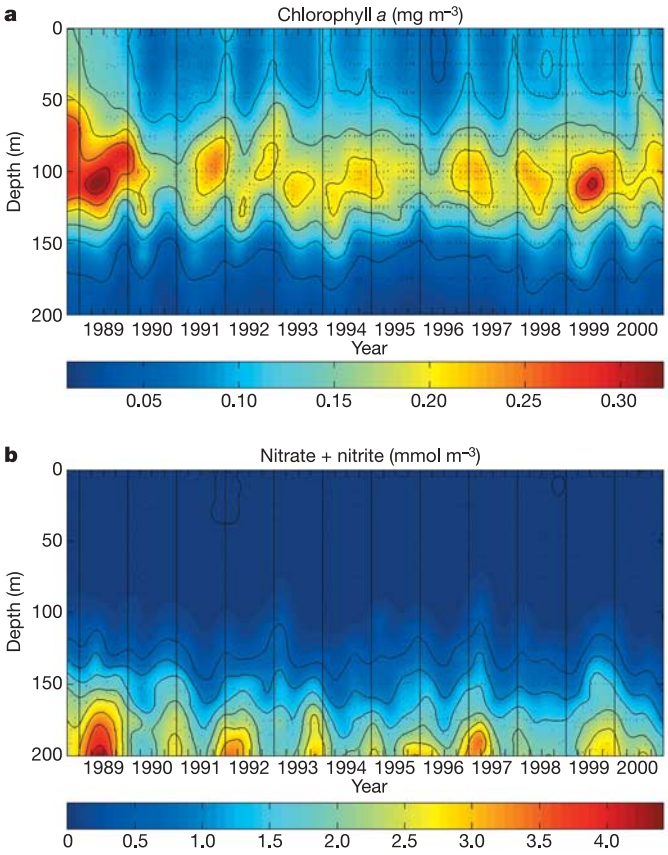

Figure 1 | Time course of the DCM at Station ALOHA, in the subtropical Pacific Ocean, North of Hawaii. a, Chlorophyll *a*. **b**, Nitrate and nitrite. Data were obtained from the Hawaii Ocean Time-series (HOT) program.

[1]Aquatic Microbiology, Institute for Biodiversity and Ecosystem Dynamics, University of Amsterdam, Nieuwe Achtergracht 127, 1018 WS Amsterdam, The Netherlands. [2]Center for Mathematics and Computer Science (CWI), PO Box 94079, 1090 GB Amsterdam, The Netherlands. [3]School of Ocean and Earth Science and Technology, University of Hawaii, 1000 Pope Road, Honolulu, Hawaii 96822, USA.
*These authors contributed equally to this work.

assume that light intensity, I, decreases exponentially with depth according to Lambert–Beer's law, owing to light absorption by the phytoplankton population, by water and by dissolved substances[15,16]. To complete the model, we use zero-flux boundary conditions for the phytoplankton. Furthermore, we assume a zero-flux boundary condition for nutrients at the surface, while nutrients are replenished from below with a fixed concentration N_B at the bottom of the water column. The model formulation and simulation methods are described in further detail in the Supplementary Information. The model is parameterized for clear ocean water, reflecting the North Pacific subtropical gyre[5,18] (Fig. 1).

In a first model simulation, with a turbulent diffusivity of $0.5\,cm^2\,s^{-1}$, nutrients in the top layer are gradually depleted by the phytoplankton. The nutricline slowly moves downwards, tracked by the phytoplankton population, until the population settles at a stable equilibrium at which the downward flux of consumed nutrients equals the upward flux of new nutrients (Fig. 2a). Thus, a stable DCM develops. For lower values of turbulent diffusivity, however, the model predicts that the phytoplankton population in the DCM will oscillate. Depending on the parameter settings, fluctuations in the DCM can range from mild oscillations (Fig. 2b) to pronounced chlorophyll peaks (Fig. 2c). To investigate this phenomenon further, we ran numerous simulations using a wide range of turbulent diffusivities. For comparison, vertical turbulent diffusivities in the ocean interior are typically on the order of $0.1\,cm^2\,s^{-1}$ to $1\,cm^2\,s^{-1}$ (refs. 19–21). The model simulations predict that the DCM becomes unstable when turbulent diffusivity is in the lower end of the realistic range (Fig. 3a). By a cascade of period doublings, reduced turbulent mixing can even generate chaos in the DCM (Fig. 3b).

The mechanism underlying these fluctuations is a difference in timescale between the sinking flux of phytoplankton and the upward diffusive flux of nutrients. This might be called an 'advection–diffusion instability'. At low diffusivity, the phytoplankton sink fast compared to the slow upward flux of nutrients. Thereby, the light conditions of the sinking phytoplankton deteriorate and the phytoplankton population declines. The declining phytoplankton population loses control over the upward nutrient flux, allowing new nutrients to diffuse further upwards. The upward flux of nutrients reaches a depth at which light conditions are suitable for growth. This fuels the next peak in the DCM. Indeed, model simulations indicate that the sinking flux has an important role in these oscillations, as oscillations were not observed with neutrally buoyant phytoplankton (results not shown). The period and amplitude of the DCM oscillations increase with increasing phytoplankton sinking velocity (Fig. 3c). The period and amplitude decrease with increasing vertical diffusivity (Fig. 3d). Thus, the oscillations become more pronounced if the timescale of sinking is fast compared to the timescale of the upward flux of nutrients.

Detailed ocean time series indicate that seasonal changes in light conditions have a large effect on the dynamics of DCMs[5] (see also Fig. 1). To add more realism to the model, we therefore forced the model by seasonal changes in incident light intensity typical for the North Pacific subtropical gyre[5], with a winter minimum of $30\,mol\,photons\,m^{-2}\,d^{-1}$ and a summer maximum of $60\,mol\,photons\,m^{-2}\,d^{-1}$. At high turbulent diffusivity, the DCM tracks the seasonal changes in light conditions (Fig. 2d). When turbulent diffusivity is reduced, the DCM exhibits a phenomenon known as phase locking, in which oscillations are squeezed within the seasonal cycle (Fig. 2e). For even lower turbulent diffusivities, seasonal forcing generates irregular phytoplankton blooms with chaotic multi-annual variability (Fig. 2f). Thus, similar to findings for other nonlinear oscillators[22,23], fluctuating DCMs show even more complex dynamics in a seasonal environment than in a constant environment.

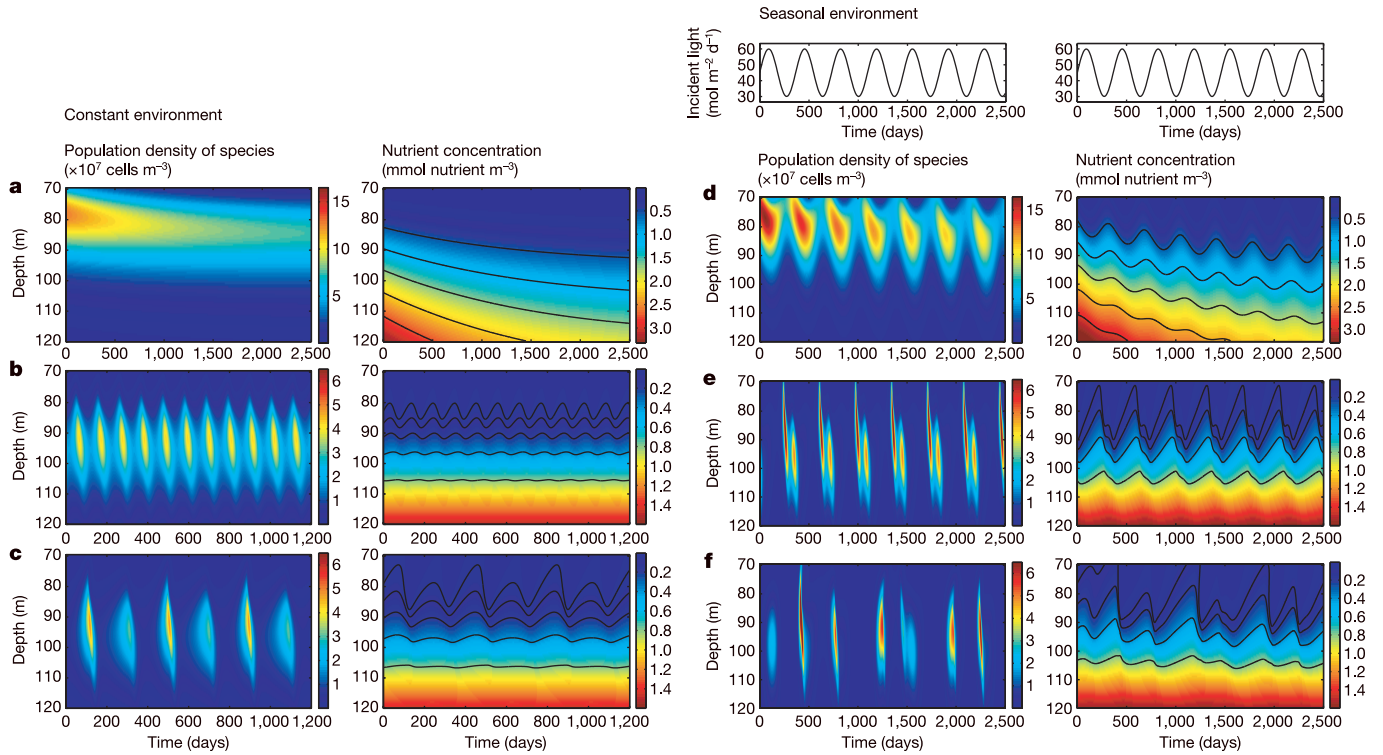

Figure 2 | Model simulations at different intensities of vertical mixing. **a–c**, Constant environment. **a**, Stable DCM ($\kappa = 0.50\,cm^2\,s^{-1}$). **b**, Mild oscillations in the DCM ($\kappa = 0.20\,cm^2\,s^{-1}$). **c**, Large-amplitude oscillations in the DCM, with double periodicity ($\kappa = 0.12\,cm^2\,s^{-1}$). **d–f**, Seasonal environment, in which the model is forced by seasonal changes in incident light intensity[5]. **d**, DCM tracks seasonal variability ($\kappa = 0.50\,cm^2\,s^{-1}$). **e**, Double periodicity of DCM locked in a seasonal environment ($\kappa = 0.14\,cm^2\,s^{-1}$). **f**, Chaotic DCM in a seasonal environment ($\kappa = 0.08\,cm^2\,s^{-1}$). For **a–f**, the left panel shows phytoplankton dynamics (P) and the right panel shows nutrient dynamics (N). See Supplementary Information for parameter values.

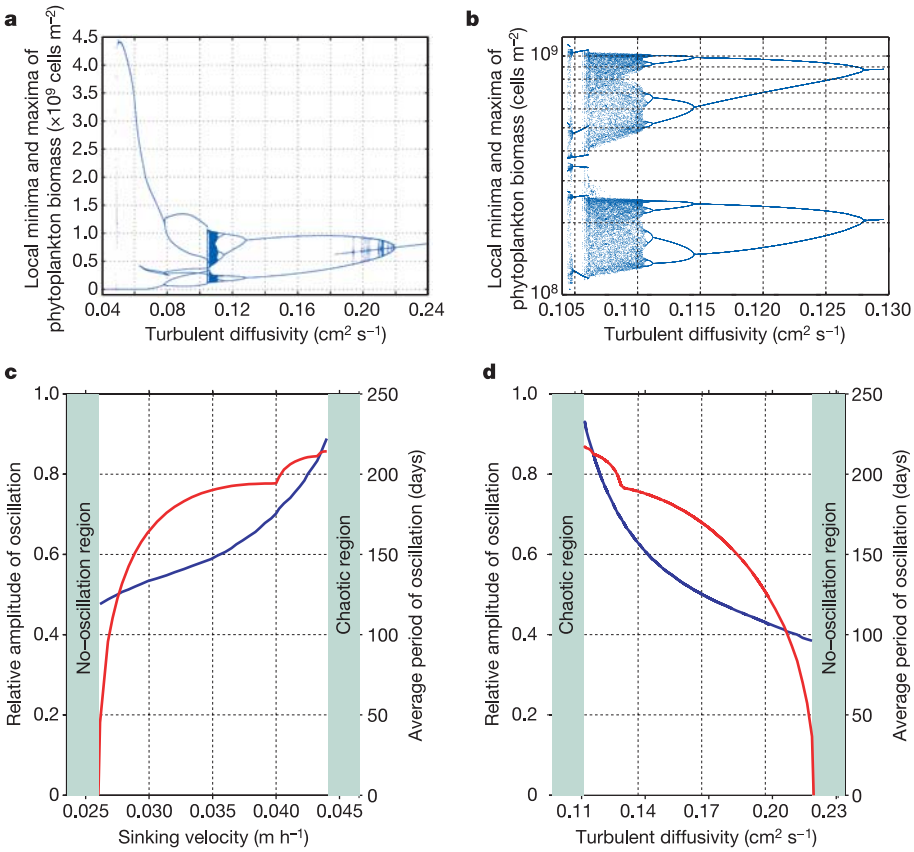

Figure 3 | Bifurcation patterns generated in a constant environment. **a**, Bifurcation diagram showing the local minima and maxima of the phytoplankton population as a function of turbulent diffusivity. **b**, Detail of the chaotic region in the bifurcation diagram. **c**, The period (blue line) and relative amplitude (red line) of the oscillations increase with phytoplankton sinking velocity. **d**, The period (blue line) and relative amplitude (red line) of the oscillations decrease with vertical turbulent diffusivity. In **a** and **b** phytoplankton population density is integrated over the upper 300 m of the water column. See Supplementary Information for parameter values.

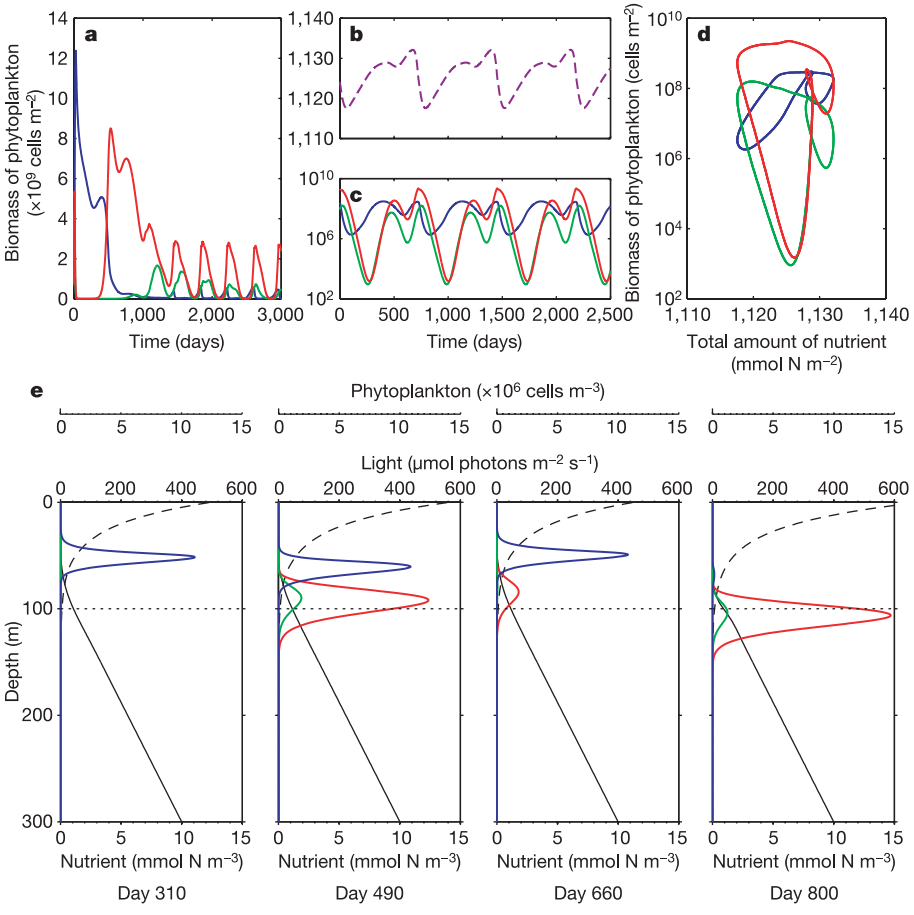

Figure 4 | Competition between three phytoplankton species in an oscillating DCM. The model (with $\kappa = 0.12\,\mathrm{cm^2\,s^{-1}}$) is forced by the same seasonal changes in incident light intensity as in Fig. 2d–f. **a**, Initial time course of the phytoplankton species. **b**, **c**, In the long run, the nutrient concentration (**b**) and the phytoplankton species (**c**) settle at a periodic attractor. **d**, Phase plane illustrating the periodic attractor of the phytoplankton species. **e**, Time series of consecutive depth profiles within a single period. Coloured lines show depth profiles of the three phytoplankton species, dashed line shows light intensity, black line shows nutrient concentration. In **a**–**d** phytoplankton population density and nutrient concentration are integrated over the upper 300 m of the water column. See Supplementary Information for parameter values.

In reality, DCMs consist of multiple phytoplankton species with different growth rates, nutrient and light requirements, and sinking velocities. How would such a diverse assemblage respond to fluctuations in the DCM? To address this issue, we developed a multi-species version of our DCM model, analogous to earlier phytoplankton competition models[16,24]. The model is again forced by seasonal changes in incident light intensity. An example is shown in Fig. 4, where we assume that the blue species has a lower sinking velocity ($0.1\ m\ d^{-1}$; resembling pico- and nanoplankton) than the red and green species ($1\ m\ d^{-1}$; resembling sinking diatoms). Furthermore, the blue species is a better nutrient competitor, whereas the red and green species are better competitors for light. Simulations show that all three species persist in this non-equilibrium environment, which confirms earlier notions that oscillations and chaos promote phytoplankton biodiversity[25]. Periods with co-dominance of the three species are alternated with periods in which either the blue species or the red and green species dominate (Fig. 4e). Furthermore, there is a subtle but consistent vertical zonation, with the blue species (better nutrient competitor) inhabiting the nutrient-depleted upper zone of the DCM, while the red and green species (superior light competitors) peak several metres deeper in the light-deprived part of the DCM. The model predicts that phytoplankton species with relatively high sinking velocities (red and green species) show larger fluctuations than small phytoplankton species with low sinking velocities (blue species; Fig. 4c–e).

Although simple models can offer only abstractions of real-world phenomena, our model adequately reproduces many features of real-world DCMs. First, the model predicts that DCMs form at a similar depth of ~100 m and span a similar depth range as observed in clear ocean waters[14] (Figs 1, 2). Second, consistent with observations, the model predicts that nutrients are depleted to near-zero levels above the DCM while the nutrient concentration increases linearly with depth below the DCM[14] (Fig. 4e). Third, detailed ocean time-series measurements from the subtropical North Pacific confirm the prediction of a vertical zonation of species, with different species assemblages dominating at different depths[26] (Supplementary Information). Fourth, these ocean time series confirm the prediction that the seasonal light cycle gives rise to seasonal patterns in chlorophyll and nutrient concentrations in the DCM[5] (Fig. 1). Fifth, the time series support the idea that plankton populations in the DCM show additional fluctuations superimposed upon the seasonal cycle, often with multi-annual variability in phytoplankton biomass and species composition[5,18,26] (Supplementary Information). Sixth, as predicted by the model, the time series tentatively suggest that phytoplankton species with relatively high sinking velocities show larger variability than phytoplankton species with low sinking velocities (Supplementary Information). In total, time-series data support the theoretical prediction that deep chlorophyll maxima can show sustained non-equilibrium dynamics, driven by a combination of external forces and the complex internal dynamics of DCMs.

Climate models predict that global warming will increase the stability of the vertical stratification in large parts of the oceans[8,9]. This will reduce vertical mixing and suppress the upward flux of nutrients, leading to a decline in oceanic primary production[9–11]. Our model predicts that the same process of reduced vertical mixing may induce oscillations and chaos in the phytoplankton of the DCM, generated by the difference in timescale between the sinking flux of phytoplankton and the upward flux of nutrients. Thus, counter-intuitively, increased stability of the water column due to global warming may destabilize the phytoplankton dynamics in the DCM, with implications for oceanic primary production, species composition and carbon export.

Received 18 July; accepted 21 September 2005.

1. Venrick, E. L., McGowan, J. A. & Mantyla, A. W. Deep maxima of photosynthetic chlorophyll in the Pacific Ocean. *Fishery Bull.* **71,** 41–52 (1973).
2. Cullen, J. J. The deep chlorophyll maximum: comparing vertical profiles of chlorophyll *a*. *Can. J. Fish. Aquat. Sci.* **39,** 791–803 (1982).
3. Mann, K. H. & Lazier, J. R. N. *Dynamics of Marine Ecosystems* (Blackwell Science, Oxford, 1996).
4. Longhurst, A. R. *Ecological Geography of the Sea* (Academic, San Diego, 1998).
5. Letelier, R. M., Karl, D. M., Abbott, M. R. & Bidigare, R. R. Light driven seasonal patterns of chlorophyll and nitrate in the lower euphotic zone of the North Pacific Subtropical Gyre. *Limnol. Oceanogr.* **49,** 508–519 (2004).
6. Venrick, E. L. Phytoplankton seasonality in the central North Pacific: the endless summer reconsidered. *Limnol. Oceanogr.* **38,** 1135–1149 (1993).
7. Holm-Hansen, O. & Hewes, C. D. Deep chlorophyll-*a* maxima (DCMs) in Antarctic waters. I. Relationships between DCMs and the physical, chemical, and optical conditions in the upper water column. *Polar Biol.* **27,** 699–710 (2004).
8. Sarmiento, J. L., Hughes, T. M. C., Stouffer, R. J. & Manabe, S. Simulated response of the ocean carbon cycle to anthropogenic climate warming. *Nature* **393,** 245–249 (1998).
9. Bopp, L. *et al.* Potential impact of climate change on marine export production. *Glob. Biogeochem. Cycles* **15,** 81–99 (2001).
10. Sarmiento, J. L. *et al.* Response of ocean ecosystems to climate warming. *Glob. Biogeochem. Cycles* **18,** doi:10.1029/2003GB002134 (2004).
11. Schmittner, A. Decline of the marine ecosystem caused by a reduction in the Atlantic overturning circulation. *Nature* **434,** 628–633 (2005).
12. Fennel, K. & Boss, E. Subsurface maxima of phytoplankton and chlorophyll: steady-state solutions from a simple model. *Limnol. Oceanogr.* **48,** 1521–1534 (2003).
13. Hodges, B. A. & Rudnick, D. L. Simple models of steady deep maxima in chlorophyll and biomass. *Deep-Sea Res. I* **51,** 999–1015 (2004).
14. Klausmeier, C. A. & Litchman, E. Algal games: the vertical distribution of phytoplankton in poorly mixed water columns. *Limnol. Oceanogr.* **46,** 1998–2007 (2001).
15. Huisman, J., Arrayás, M., Ebert, U. & Sommeijer, B. How do sinking phytoplankton species manage to persist? *Am. Nat.* **159,** 245–254 (2002).
16. Huisman, J. *et al.* Changes in turbulent mixing shift competition for light between phytoplankton species. *Ecology* **85,** 2960–2970 (2004).
17. Okubo, A. & Levin, S. A. *Diffusion and Ecological Problems: Modern Perspectives* 2nd edn (Springer, Berlin, 2001).
18. Karl, D. M. *et al.* Seasonal and interannual variability in primary production and particle flux at Station ALOHA. *Deep-Sea Res. II* **43,** 539–568 (1996).
19. Lewis, M. R., Harrison, W. G., Oakey, N. S., Hebert, D. & Platt, T. Vertical nitrate fluxes in the oligotrophic ocean. *Science* **234,** 870–873 (1986).
20. Smyth, W. D., Moum, J. N. & Caldwell, D. R. The efficiency of mixing in turbulent patches: inferences from direct simulations and microstructure observations. *J. Phys. Oceanogr.* **31,** 1969–1992 (2001).
21. Finnigan, T. D., Luther, D. S. & Lukas, R. Observations of enhanced diapycnal mixing near the Hawaiian ridge. *J. Phys. Oceanogr.* **32,** 2988–3002 (2002).
22. Rinaldi, S., Muratori, S. & Kuznetsov, Y. Multiple attractors, catastrophes and chaos in seasonally perturbed predator-prey communities. *Bull. Math. Biol.* **55,** 15–35 (1993).
23. Vandermeer, J., Stone, L. & Blasius, B. Categories of chaos and fractal basin boundaries in forced predator-prey models. *Chaos Soliton Fract.* **12,** 265–276 (2001).
24. Huisman, J. & Sommeijer, B. Population dynamics of sinking phytoplankton in light-limited environments: simulation techniques and critical parameters. *J. Sea Res.* **48,** 83–96 (2002).
25. Huisman, J. & Weissing, F. J. Biodiversity of plankton by species oscillations and chaos. *Nature* **402,** 407–410 (1999).
26. Venrick, E. L. Phytoplankton species structure in the central North Pacific, 1973–1996: variability and persistence. *J. Plankton Res.* **21,** 1029–1042 (1999).

Supplementary Information is linked to the online version of the paper at www.nature.com/nature.

Acknowledgements We thank R. R. Bidigare for HPLC pigment analyses, and M. Stomp, J.G. Verwer and J. Williams for discussions. J.H. was supported by the Earth and Life Sciences Foundation (ALW), which is subsidized by the Netherlands Organization for Scientific Research (NWO). N.N.P.T. was supported by the Computational Science program of NWO. D.M.K. acknowledges support from the US National Science Foundation and the Gordon and Betty Moore Foundation. B.S. acknowledges support from the Dutch BSIK/BRICKS project.

Author Contributions J.H. and N.N.P.T. contributed equally to this work. J.H., N.N.P.T. and B.S. developed the model structure. N.N.P.T. and B.S. wrote the numerical code. D.M.K. provided data from the Hawaii Ocean Time-series program. J.H. wrote the paper. All authors discussed the results and commented on the manuscript.

Author Information The time-series data from the Hawaii Ocean Time-series program are deposited at http://hahana.soest.hawaii.edu/hot/hot-dogs. Reprints and permissions information is available at npg.nature.com/reprintsandpermissions. The authors declare no competing financial interests. Correspondence and requests for materials should be addressed to J.H. (jef.huisman@science.uva.nl).